Journal of Peptide Science
J. Peptide Sci. **6**: 571–583 (2000)

Preferred Conformation of Peptides Based on Cycloaliphatic $C^{\alpha,\alpha}$-disubstituted Glycines: 1-Amino-cycloundecane-1-carboxylic Acid ($Ac_{11}c$)

MICHELE SAVIANO[a], ROSA IACOVINO[b], ETTORE BENEDETTI[a], VITTORIO MORETTO[c], ALESSANDRO BANZATO[c], FERNANDO FORMAGGIO[c], MARCO CRISMA[c] and CLAUDIO TONIOLO[c,*]

[a] Biocrystallography Research Centre, CNR, Department of Chemistry, University of Naples 'Federico II', 80134 Napoli, Italy
[b] Department of Environmental Sciences, Second University of Naples, 81100 Caserta, Italy
[c] Biopolymer Research Centre, CNR, Department of Organic Chemistry, University of Padova, 35131 Padova, Italy

Received 22 March 2000
Accepted 10 July 2000

Abstract: Two complete series of N-protected oligopeptide esters to the pentamer level from 1-amino-cycloundecane-1-carboxylic acid ($Ac_{11}c$), an α-amino acid conformationally constrained through a medium-ring $C^{\alpha}_{i} \leftrightarrow C^{\alpha}_{i}$ cyclization, and either the L-Ala or Aib residue, along with the N-protected $Ac_{11}c$ monomer and homo-dimer alkylamides, have been synthesized by solution methods and fully characterized. The preferred conformation of these model peptides has been assessed in deuterochloroform solution by FT-IR absorption and ^{1}H-NMR techniques. Furthermore, the molecular structures of one derivative (Z-$Ac_{11}c$-OH) and two peptides (the tripeptide ester Z-Aib-$Ac_{11}c$-Aib-O*t*Bu and the pentapeptide ester Z-$Ac_{11}c$-$(Aib)_2$-$Ac_{11}c$-Aib-O*t*Bu) have been determined in the crystal state by X-ray diffraction. The experimental results support the view that β-bends and 3_{10}-helices are preferentially adopted by peptides rich in $Ac_{11}c$, the second largest cycloaliphatic $C^{\alpha,\alpha}$-disubstituted glycine known. This investigation has allowed the authors to approach the completion of a detailed conformational analysis of the whole 1-amino-cycloalkane-1-carboxylic acid (Ac_nc, with $n = 3$–12) series, which represents the prerequisite for their recent proposal of the 'Ac_nc scan' concept.

Keywords: β-bend; cyclic amino acid; 3_{10}-helix; peptide conformation; X-ray diffraction

INTRODUCTION

Medicinal chemists have frequently faced the problem of discovering small molecules that mimic pharmacological profiles of bioactive peptides. To stabilize an appropriate conformation and reduce enzymatic hydrolysis, geometrical constraints have often been introduced in peptidomimetic compounds. Among the various types of recently proposed *stepping stones* to facilitate the design of small bioactive molecules, $C^{\alpha,\alpha}$-disubstituted glycines have proven to be of great value [1–11]. In this connection the prototypical α-amino acid of this class (Aib) [12–16] is known to strongly favour β-bend [17–19] and 3_{10}-/α-helical structures [20]. Similarly folded conformations are also typically observed in peptides rich in other α-amino acids of this class, more specifically those with $C^{\alpha}_{i} \leftrightarrow C^{\alpha}_{i}$ cyclization (1-aminocycloalkane-1-carboxylic acids, Ac_nc, with $n = 3$–9, 12) [4,14,16,21,22].

Abbreviations: Ac_nc, 1-aminocycloalkane-1-carboxylic acid; Aib, α-aminoisobutyric acid or $C^{\alpha,\alpha}$-dimethylglycine; O*t*Bu, *tert*-butoxy; NHiPr, isopropylamino; TEMPO, 2,2,6,6-tetramethylpiperidinyl-1-oxy; Z, benzyloxycarbonyl.

* Correspondence to: Biopolymer Research Centre, CNR, Department of Organic Chemistry, University of Padova, Via Marzolo 1, 35131 Padova, Italy; e-mail: biop02@chor.unipd.it

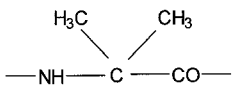

Aib

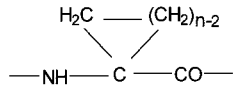

Ac_nc

The present conformational analysis of $Ac_{11}c$ in selected model peptides was carried out with the aim at expanding the available general picture of the geometrical and structural preferences of the Ac_nc residues. In this paper the synthesis, characterization and solution conformational study (by FT-IR absorption and ^{1}H-NMR techniques) of two complete series of terminally protected $Ac_{11}c$/L-Ala and $Ac_{11}c$/Aib oligopeptides are reported. The results are corroborated by those on the $Ac_{11}c$ monomer and homo-dimer alkylamides. One derivate and two peptides gave single crystals which were investigated by X-ray diffraction. Preliminary accounts of a limited part of this work have been reported elsewhere [23].

MATERIALS AND METHODS

Synthesis and Characterization of Peptides

Melting points were determined using a Leitz (Wetzlar, Germany) model Laborlux 12 apparatus and are not corrected. Optical rotations were measured using a Perkin–Elmer (Norwalk, CT, USA) model 241 polarimeter equipped with a Haake (Karlsruhe, Germany) model D thermostat. Thin-layer chromatography (TLC) was performed on Merck (Darmstadt, Germany) Kieselgel $60F_{254}$ precoated plates using the following solvent systems: 1 ($CHCl_3$–EtOH, 9:1), 2 (Bu^nOH–AcOH–H_2O, 3:1:1), 3 (toluene–EtOH, 7:1). The chromatograms were examined by UV fluorescence or developed by chlorine–starch–potassium iodide or ninhydrin chromatic reaction as appropriate. All the compounds were obtained in a chromatographically homogeneous state.

Infrared Absorption

The solid-state infrared absorption spectra (KBr disc technique) were recorded with a Perkin–Elmer model 580 B spectrophotometer equipped with a Perkin–Elmer model 3600 IR data station and a model 660 printer. The solution spectra were obtained using a Perkin–Elmer model 1720 X FT-IR spectrophotometer, nitrogen flushed, equipped with a sample-shuttle device, at 2 cm^{-1} nominal resolution, averaging 100 scans. Cells with path lengths of 0.1, 1.0 and 10 mm (with CaF_2 windows) were used. Spectrograde deuterochloroform (99.8%, d) was purchased from Merck (Darmstadt, Germany). Solvent (baseline) spectra were recorded under the same conditions.

^{1}H-NMR

The ^{1}H-NMR spectra were recorded with a Bruker (Karlsruhe, Germany) model AM 400 spectrometer. Measurements were carried out in deuterochloroform (99.96% d; Aldrich, Milwaukee, WI, USA) and deuterated dimethylsulfoxide (DMSO) (99.96% d_6; Stohler, Waltham, MA, USA) with tetramethylsilane as the internal standard. The free radical 2,2,6,6-tetramethylpiperidinyl-1-oxy (TEMPO) was purchased from Sigma (St Louis, MO, USA).

X-Ray Diffraction

Colourless single crystals of the amino acid derivative Z-$Ac_{11}c$OH, the tripeptide Z-Aib-$Ac_{11}c$-Aib-O*t*Bu, and the pentapeptide Z-$Ac_{11}c$-$(Aib)_2$-$Ac_{11}c$-Aib-O*t*Bu were grown by slow evaporation at room temperature from the solvents reported in Table 1. Data collections were carried out on a CAD4 Enraf-Nonius X-ray diffractometer of the Biocrystallography Research Center, CNR, at the University of Naples 'Federico II'. Unit cell determinations were carried out for all crystals by least-square refinement of the setting angles of 25 high angle reflections accurately centred. No significant variation was observed in the intensities of the standard reflections monitored at regular intervals during data collection, thus implying electronics and crystal stabilities. Lorentz and polarization corrections were applied to the intensities, but no absorption correction was made. Crystallographic data for the three compounds are listed in Table 1.

The three structures were solved by direct methods using the program SIR97 [24]. The solution with the best figure of merit revealed the coordinates of most of the non-hydrogen atoms; the remaining ones and the statistical disorder for the ring of Z-$Ac_{11}c$-OH and of molecule **B** of the tripeptide were recovered using difference Fourier techniques. Refinement of the three structures was performed by full-matrix least-squares procedures with the program SHELXL97 [25]. The occupancy factors for the statistical side-chain atoms $C_1^{\zeta 2}$ of Z-$Ac_{11}c$-OH and $C_2^{\gamma 2}$ of molecule **B** of the tripeptide were refined and their final value was in both cases 0.5. All non-H atoms were refined anisotropically. H-atoms of the three compounds were calculated and during the

Table 1 Crystallographic Data for the $Ac_{11}c$ Derivative and Peptides

	Z-$Ac_{11}c$-OH	Z-Aib-$Ac_{11}c$-Aib-O*t*Bu	Z-$Ac_{11}c$-$(Aib)_2$-$Ac_{11}c$-Aib-O*t*Bu
Empirical formula	$C_{20}H_{29}NO_4$	$C_{32}H_{51}N_3O_6$	$C_{48}H_{79}N_5O_8$
Formula weight (a.m.u.)	347.4	573.8	854.2
Crystal system	Monoclinic	Monoclinic	Triclinic
Space group	$P2_1/n$	$P2_1/n$	$P\bar{1}$
a (Å)	16.736(5)	22.164(4)	11.195(1)
b (Å)	10.478(2)	19.129(4)	12.674(4)
c (Å)	14.276(2)	17.066(5)	18.607(7)
α (°)	90	90	103.5(1)
β (°)	129.8(1)	109.5(1)	99.3(1)
γ (°)	90	90	96.8(1)
V (Å^3)	1922(1)	6819(3)	2499(1)
Z (molecules/unit cell)	4	8	2
Density (calc.) (g/cm^3)	1.203	1.117	1.139
Independent reflections	3528	12902	9475
Observed reflections	2051 [$I>2\sigma(I)$]	6707 [$I>2\sigma(I)$]	7258 [$I>2\sigma(I)$]
Solved by	SIR97 [24]	SIR97	SIR97
Refined by	SHELX97 [25]	SHELX97	SHELX97
S	1.090	1.437	1.130
Final R indices [$I>2\sigma(I)$]	$R_1 = 0.0720$, $wR_2 = 0.207$	$R_1 = 0.0825$, $wR_2 = 0.234$	$R_1 = 0.0771$, $wR_2 = 0.233$
R indices (all data)	$R_1 = 0.1188$, $wR_2 = 0.244$	$R_1 = 0.1341$, $wR_2 = 0.269$	$R_1 = 0.0912$, $wR_2 = 0.255$
Temperature (K)	293	293	293
Radiation (λ, Å)	Cu Kα (1.54178 Å)	Cu Kα (1.54178 Å)	Cu Kα (1.54178 Å)
Scan method	θ /2θ	θ /2θ	θ /2θ
θ range (°)	1–70	1–70	1–70
Crystallization solvent	EtOAc/petroleum ether	$CHCl_3$/petroleum ether	$CHCl_3$/petroleum ether
Crystal size (mm)	$0.5\times0.2\times0.3$	$0.5\times0.3\times0.3$	$0.2\times0.3\times0.3$
$\Delta\rho_{max}$ and $\Delta\rho_{min}$	0.461/−0.207	0.450/−0.319	0.236/−0.208

refinement they were allowed to ride on their carrying atoms, with U_{iso} set equal to 1.2 times the U_{eq} of the attached atom.

The scattering factors for all atomic species were calculated from Cromer and Waber [26]. Further details of the crystal structures, including final atomic parameters for the non-H atoms, have been deposited with and are available on request from the Director of the Cambridge Crystallographic Data Centre, 12 Union Road, Cambridge CB2 1EZ, UK, on quoting the full journal citation.

RESULTS

Synthesis of $Ac_{11}c$ and Its Derivatives and Peptides

$Ac_{11}c$ amide hydrochloride was prepared by treatment of cycloundecanone with sodium cyanide, acetic acid, and excess of ammonia, and subsequent acid hydrolysis (HCl/HCOOH at 0–20°C) of the α-aminonitrile intermediate (Strecker synthesis). A more drastic acid hydrolysis (6 N HCl, under reflux) of $Ac_{11}c$ amide hydrochloride afforded the free amino acid [27].

The Z-protected L-Ala and Aib derivatives were synthesized by treatment of the free amino acid with Z-Cl in an acetone–water (pH 10.9) mixture. The Z-protected $Ac_{11}c$ derivative was obtained by reacting the free amino acid with *N*-(benzyloxycarbonyloxy)-succinimide in acetonitrile in the presence of tetramethylammonium hydroxide. The Z-protected L-Ala and Aib *tert*-butyl esters were prepared by treatment of the corresponding N-protected amino acids with isobutene in methylene chloride in the presence of a catalytic amount of sulphuric acid. The symmetrical anhydride (Z-Aib)$_2$O was synthesized in acetonitrile by intermolecular dehydration of the N-protected amino acid with *N*-ethyl,*N*′-(3-dimethylaminopropyl)-carbodiimide in a 2:1 molar ratio.

Table 2 Physical and Analytical Properties for $Ac_{11}c$, its Derivatives and Peptides

Compound	Melting point (°C)	Recrystallization solvent[a]	$[\alpha]_D^{20}$ (°)[b]	TLC			IR[c] (cm^{-1})
				R_{FI}	R_{FII}	R_{FIII}	
H-Ac_{11}c-OH	>340	DE[d]	—	0.05	0.75	0.00	3443, 1627, 1584, 1520
HCl · H-Ac_{11}c-NH_2	243–245	DE[d]	—	0.40	0.70	0.10	3358, 1684, 1509
Z-Ac_{11}c-OH	150–151	EtOAc/LP	—	0.85	0.95	0.25	3372, 1716, 1695, 1585, 1526
Z-Ac_{11}c-NHiPr	192–194	EtOAc/LP	—	0.80	0.95	0.25	3310, 1696, 1650,1587, 1535
Z-(Ac_{11}c)$_2$-NHiPr	196–198	EtOAc/LP	—	0.95	0.95	0.35	3426, 3320, 1704, 1648, 1584, 1527
Z-Ac_{11}c-L-Ala-O*t*Bu	127–128	EtOAc/LP	−14.1	0.90	0.95	0.70	3313, 1738, 1693, 1650, 1584, 1528
Z-L-Ala-Ac_{11}c-L-Ala-O*t*Bu	203–204	EtOAc/LP	−26.6	0.70	0.95	0.45	3385, 3297, 1740, 1703, 1677, 1641, 1538
Z-Ac_{11}c-(L-Ala)$_2$-O*t*Bu	165–166	EtOAc/LP	−32.6	0.70	0.95	0.45	3318, 1733, 1693, 1645, 1529
Z-(L-Ala)$_2$-Ac_{11}c-L-Ala-O*t*Bu	177–178	EtOAc/LP	−32.5	0.55	0.95	0.35	3315, 1725, 1707, 1657, 1529
Z-Ac_{11}c-(L-Ala)$_2$-Ac_{11}c-L-Ala-O*t*Bu	164–166	EtOAc/LP	−0.9	0.55	0.95	0.20	3321, 1728, 1660, 1532
Z-Ac_{11}c-Aib-O*t*Bu	173–174	EtOAc/LP	—	0.95	0.95	0.70	3389, 3291, 1720, 1647, 1583, 1534
Z-Aib-Ac_{11}c-Aib-O*t*Bu	181–182	EtOAc/LP	—	0.75	0.95	0.40	3431, 3344, 1734, 1704, 1685, 1649, 1528
Z-(Aib)$_2$-Ac_{11}c-Aib-O*t*Bu	226–227	EtOAc/LP	—	0.60	0.95	0.25	3434, 3335, 1733, 1702, 1678, 1655, 1584, 1529
Z-Ac_{11}c-(Aib)$_2$-Ac_{11}c-Aib-O*t*Bu	266–267	EtOAc/LP	—	0.75	0.95	0.30	3410, 3312, 1721, 1698, 1662, 1529

[a] DE, diethyl ether; EtOAc, ethyl acetate; LP, light petroleum.
[b] $c = 0.5$, methanol.
[c] The IR absorption spectra were obtained in KBr pellets (only significant bands in the 3500–3200 and 1850–1500 cm^{-1} regions are reported).
[d] The solid compound was washed with this solvent.

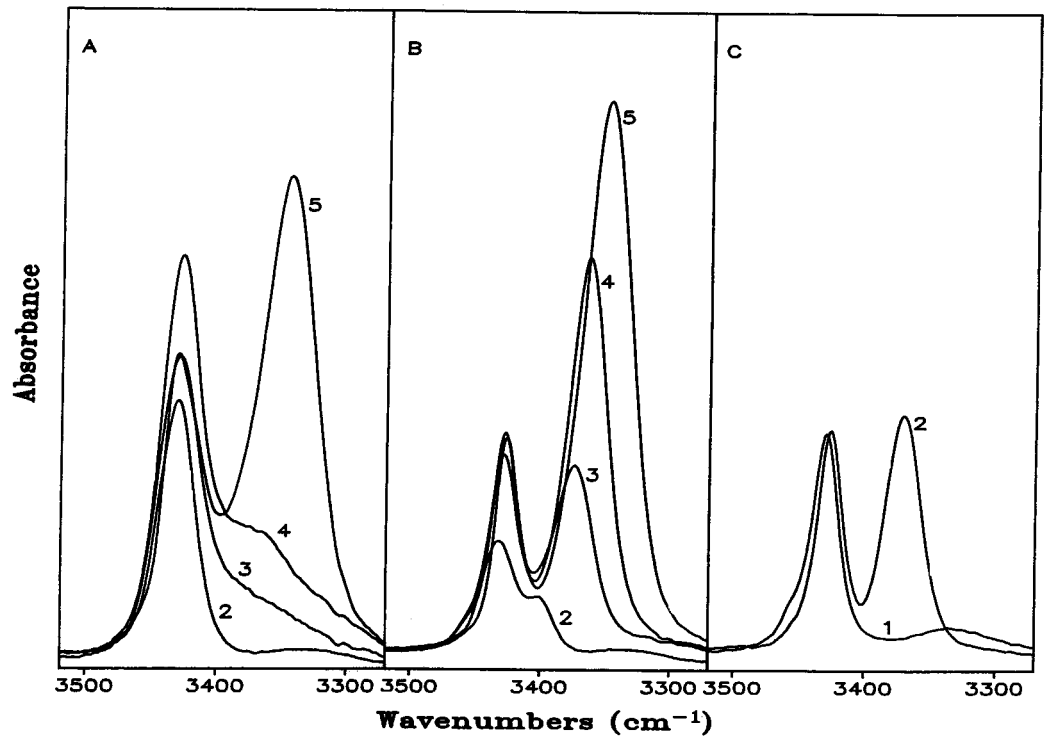

Figure 1 FT-IR absorption spectra (N–H stretching region) of (A) Z-$Ac_{11}c$-L-Ala-O*t*Bu (2), Z-L-Ala-$Ac_{11}c$-L-Ala-O*t*Bu (3), Z-(L-Ala)$_2$-$Ac_{11}c$-L-Ala-O*t*Bu (4), and Z-$Ac_{11}c$-(L-Ala)$_2$-$Ac_{11}c$-L-Ala-O*t*Bu (5); (B) Z-$Ac_{11}c$-Aib-O*t*Bu (2), Z-Aib-$Ac_{11}c$-Aib-O*t*Bu (3), Z-(Aib)$_2$-$Ac_{11}c$-Aib-O*t*Bu (4), and Z-$Ac_{11}c$-(Aib)$_2$-$Ac_{11}c$-Aib-O*t*Bu (5); (C) Z-$Ac_{11}c$-NHiPr (1) and Z-($Ac_{11}c$)$_2$-NHiPr (2) in $CDCl_3$ solution (peptide concentration 1 mM).

L-Ala-L-Ala, L-Ala-$Ac_{11}c$, $Ac_{11}c$-L-Ala, $Ac_{11}c$-Aib, $Ac_{11}c$-$Ac_{11}c$ and $Ac_{11}c$-NH alkyl peptide (amide) bond formation was obtained in methylene chloride using *N*-ethyl,*N*′-(3-dimethylaminopropyl)-carbodiimide in the presence of 7-aza-1-hydroxy-1,2,3-benzotriazole as the hydroxylamine-based additive [28]. On the other hand, formation of the Aib-Aib and Aib-$Ac_{11}c$ peptide bonds was achieved by the symmetrical anhydride method in methylene chloride. Removal of the Z-group was performed by catalytic hydrogenation in methylene chloride.

The physical properties and analytical data for $Ac_{11}c$ and its derivatives and peptides are listed in Table 2. The newly synthesized compounds were also characterized by ^{1}H-NMR (data not shown).

Solution Conformational Analysis

The conformational preferences of the $Ac_{11}c$-based peptides in solution were assessed in a structure-supporting solvent ($CDCl_3$) by FT-IR absorption and ^{1}H-NMR as a function of concentration (over the range 10–0.1 mM).

Figure 1 shows the FT-IR absorption spectra (N–H stretching region) of the terminally protected $Ac_{11}c$/L-Ala and $Ac_{11}c$/Aib peptides (to the pentapeptide level) along with those of the $Ac_{11}c$ monomer and homo-dimer alkylamides. The curves of the dipeptide amide, tripeptides and higher oligomers are characterized by two bands, at 3432–3426 cm^{-1} (free, solvated NH groups) and 3374–3345 cm^{-1} (H-bonded NH groups), respectively [29]. The intensity of the low-frequency band relative to the high-frequency band (A_H/A_F ratio) markedly increases as the main-chain length increases. Concomitantly, the absorption maximum shifts significantly to lower wavenumbers. An inspection of the spectrum of the homo-dimer alkylamide, compared to those of the -Aib-$Ac_{11}c$-Aib-, -L-Ala-$Ac_{11}c$-L-Ala-, and -$Ac_{11}c$-L-Ala-L-Ala- esters (the latter spectrum not shown), allows the determination of the rank order of the A_H/A_F ratios as follows: Z-$Ac_{11}c$-$Ac_{11}c$-NHiPr > Z-Aib-$Ac_{11}c$-Aib-O*t*Bu $\gg$ Z-$Ac_{11}c$-L-Ala-L-Ala-O*t*Bu > Z-L-Ala-$Ac_{11}c$-L-Ala-O*t*Bu. It can also be shown that, even at 10 mM concentration, there are only negligible changes in the spectra of all di-, tri-, and tetrapeptides examined (not shown). In the two pentapeptides, however, and particularly in the Aib/L-Ala compound, a

variation was observed, albeit small, in the A_H/A_F ratio. In any case, in all peptides the H-bonding band should be interpreted as arising from intramolecular N–H···O=C interactions to a very large extent.

This FT-IR absorption analysis has provided convincing evidence that main-chain length dependent intramolecular H-bonding is a factor of paramount importance in biasing a folded conformation for the N- and C-protected $Ac_{11}c$ peptides in $CDCl_3$ solution. The findings also support the view that $Ac_{11}c$ is not only a much stronger inducer of intramolecularly H-bonded conformers than a typical protein amino acid (Ala), but even slightly more effective than Aib itself.

The delineation of inaccessible (or intramolecularly H-bonded) NH groups of the terminally protected $Ac_{11}c$ peptides by ^{1}H-NMR was performed using: (i) solvent dependence of NH chemical shifts, by adding increasing amounts of the strong H-bonding acceptor solvent DMSO [30,31] to the $CDCl_3$ solution and (ii) free-radical (TEMPO) induced line broadening of NH resonances [32]. As typical examples, Figure 2 shows the behaviour of the NH resonances of the $Ac_{11}c$/L-Ala and $Ac_{11}c$/Aib pentapeptides upon addition of DMSO and TEMPO. The upfield resonances in $CDCl_3$ solution is unambiguously assigned to the *urethane* N(1)H proton [29]. In any case, complete assignments of all NH protons of the two peptides was achieved from ROESY experiments. From an analysis of the spectra as a function of concentration (10–1 mM) in $CDCl_3$ solution (spectra not shown), it could be concluded that dilution induces a negligible shift (≤ 0.02 ppm) to higher fields of all NH resonances of di-, tri- and tetrapeptides, and the N(3)H to N(5)H resonances of the pentapeptides. However, this effect become significant for the N(1)H and N(2)H resonances of the pentapeptides, where shifts of 0.08–0.12 ppm for the N(1) resonances and 0.03–0.06 ppm for the N(2)H resonances were found. In the two $Ac_{11}c$ pentapeptides investigated in the $CDCl_3$–DMSO mixtures and in the presence of the paramagnetic perturbing agent TEMPO two classes of NH protons were observed. Class (i) [N(1)H and N(2)H protons] includes protons whose chemical shifts are sensitive to the addition of DMSO and whose resonances broaden upon addition of TEMPO. Interestingly, in both peptides the sensitivity of the N(1)H protons is higher than that of the N(2) proton. Class (ii) [N(3)H to N(5)H protons] includes those displaying a behaviour characteristic of shielded protons (relative insensitivity of chemical shifts to solvent composition and of line-widths to the presence of TEMPO).

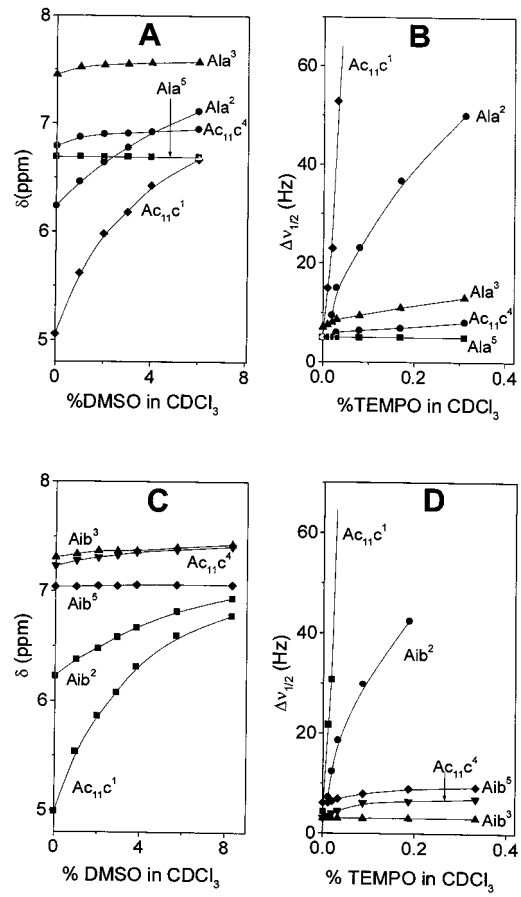

Figure 2 Plots of NH chemical shifts in the ^{1}H-NMR spectra of Z-$Ac_{11}c$-(L-Ala)$_2$-$Ac_{11}c$-L-Ala-O*t*Bu (A) and Z-$Ac_{11}c$-(Aib)$_2$-$Ac_{11}c$-Aib-O*t*Bu (C) as a function of increasing percentages of DMSO (v/v) added to the $CDCl_3$ solution. Plot of bandwidths of the NH signals in the ^{1}H-NMR spectra of Z-$Ac_{11}c$-(L-Ala)$_2$-$Ac_{11}c$-L-Ala-O*t*Bu (B) and Z-$Ac_{11}c$-(Aib)$_2$-$Ac_{11}c$-Aib-O*t*Bu (D) as a function of increasing percentages of TEMPO (w/v) added to the $CDCl_3$ solution (peptide concentration 1 mM).

To summarize, the ^{1}H-NMR results, described here, allow one to conclude that in $CDCl_3$ solution at a concentration higher than 1 mM, the $Ac_{11}c$-rich peptides have some propensity to self-aggregate and that in this process the urethane N(1)H and the peptide N(2)H protons play a major role as intermolecular H-bonding donors. At lower concentrations the N(3)H to N(5)H protons of the tri-, tetra-, and pentapeptides are almost inaccessible to perturbing agents and are, therefore, most probably, intramolecularly H-bonded. In view of these findings and by analogy with the conformational

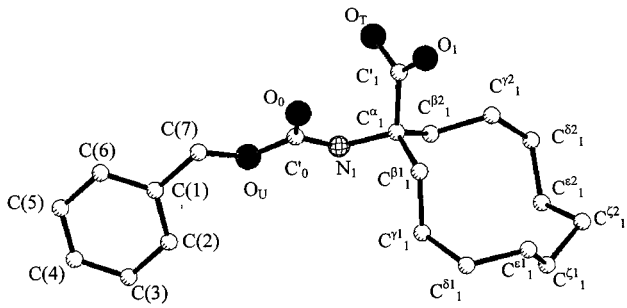

Figure 3 X-ray diffraction structure of Z-$Ac_{11}c$-OH with the atoms numbered.

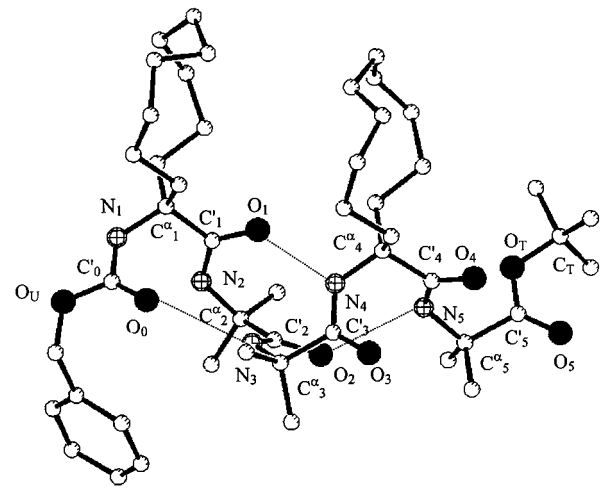

Figure 5 X-ray diffraction structure of Z-$Ac_{11}c$-$(Aib)_2$-$Ac_{11}c$-Aib-O*t*Bu with the atoms numbered (for clarity only the backbone atoms are labelled). The three intramolecular H-bonds are represented by dotted lines.

tendency of other cycloaliphatic $C^{\alpha,\alpha}$-disubstituted glycines [4,14,16,21,22], it is reasonable to conclude that the most populated structures assumed in $CDCl_3$ solution by the N- and C-protected $Ac_{11}c$ tri-, tetra- and longer peptides are the β-bend, two consecutive β-bends (incipient 3_{10}-helix), and the 3_{10}-helix, respectively. These conclusions agree well with those extracted from the FT-IR absorption investigation discussed above.

Crystal-state Conformational Analysis

The molecular and crystal structures of the following $Ac_{11}c$ derivative and peptides were elucidated by X-ray diffraction: Z-$Ac_{11}c$-OH, Z-Aib-$Ac_{11}c$-Aib-O*t*Bu (two independent molecules, **A** and **B**, in the asymmetric unit), and Z-$Ac_{11}c$-$(Aib)_2$-$Ac_{11}c$-Aib-O*t*Bu. The molecular structures with the atomic numbering schemes are illustrated in Figures 3–5, respectively. Relevant N^{α}-protecting group, backbone and side-chain torsion angles [33] are given in Table 3. In Table 4 the intra- and intermolecular H-bond parameters are listed, while the average bond lengths and bond angles characterizing the $Ac_{11}c$ residue are reported in Table 5.

Bond lengths and bond angles are in general agreement with previously reported values for the geometry of the benzyloxycarbonylamino moiety [34], the ester group [35], and the peptide unit [36,37]. The average geometry for the $Ac_{11}c$ residue has also been calculated. All parameters are close to those reported in the literature for

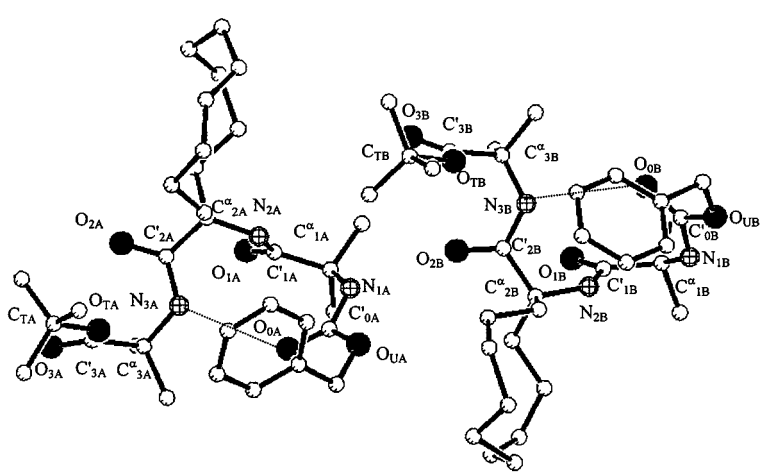

Figure 4 X-ray diffraction structure of the two independent molecules (**A** and **B**) in the asymmetric unit of Z-Aib-$Ac_{11}c$-Aib-O*t*Bu with the atoms numbered (for clarity only the backbone atoms are labelled). The intramolecular H-bond is represented by a dotted line.

Table 3 Selected N^{α}-Protecting Group, Backbone and Side-chain Torsion Angles (°) for the $Ac_{11}c$ Derivative and Peptides

Torsion angle	Z-$Ac_{11}c$-OH	Z-Aib-$Ac_{11}c$-Aib-O*t*Bu		Z-$Ac_{11}c$-$(Aib)_2$-$Ac_{11}c$-Aib-O*t*Bu
		Mol. **A**	Mol. **B**	
$\theta^{3,1}$	40.7(5)	61.2(5)	−44.3(4)	70.1(7)
$\theta^{3,2}$	−139.0(4)	−117.9(4)	136.0(5)	−109.0(7)
θ^{2}	−164.5(3)	75.6(5)	−81.2(5)	79.6(8)
θ^{1}	177.4(3)	−168.3(3)	174.3(3)	−172.3(4)
ω_0	−176.9(3)	−172.9(3)	170.4(3)	−178.0(4)
ϕ_1	−49.5(3)	−61.3(4)	61.2(5)	−58.9(6)
ψ_1	−49.2(3)[a]	−25.0(4)	26.2(5)	−24.8(6)
ω_1		−177.5(3)	178.9(3)	176.9(3)
ϕ_2		−56.2(4)	55.8(4)	−51.7(5)
ψ_2		−33.0(4)	30.2(5)	−29.4(6)
ω_2		170.7(3)	−177.7(3)	179.5(4)
ϕ_3		54.6(5)	−51.4(5)	−54.2(5)
ψ_3		52.3(4)[b]	−45.3(4)[b]	−26.1(5)
ω_3		175.4(3)[c]	−179.1(3)[c]	−179.5(3)
ϕ_4				−51.8(6)
ψ_4				−42.8(5)
ω_4				173.3(4)
ϕ_5				55.9(5)
ψ_5				45.2(6)[d]
ω_5				174.1(5)[e]
$\chi 1^{1,1}$	60.9(4)			53.0(5)
$\chi 1^{2,1}$	153.9(3)			155.8(5)
$\chi 1^{3,1}$	−70.6(5)			−96.3(8)
$\chi 1^{4,1}$	−69.8(6)			85.4(19)
$\chi 1^{5,1}$	139.0(8)			−143.8(14)
$\chi 1^{6}$	−56(3) [−106(1)][f]			68(2)
$\chi 1^{5,2}$	−41(3) [128.9(7)][f]			78(2)
$\chi 1^{4,2}$	83(2) [−79.4(8)][f]			−68.0(12)
$\chi 1^{3,2}$	−126.8(9) [−70.3(6)][f]			−65.7(13)
$\chi 1^{2,2}$	153.8(3)			151.2(9)
$\chi 1^{1,2}$	175.6(3)			174.1(4)
$\chi 2^{1,1}$		48.1(4)	−42.0(5)	
$\chi 2^{1,2}$		143.6(6)	−155.5(5)	
$\chi 2^{1,3}$		−66.0(9)	68.4(9)	
$\chi 2^{1,4}$		−61.0(13)	85.3(10)	
$\chi 2^{1,5}$		137.7(10)	−89.7(11)	
$\chi 2^{6}$		−130.2(11)	−42.2(16)	
$\chi 2^{5,2}$		127.2(9)	145.7(18)	
$\chi 2^{4,2}$		−66.7(10)	−43(3) [−104(2)][f]	
$\chi 2^{3,2}$		−61.4(8)	−104.5(10) [103.1(11)][f]	
$\chi 2^{2,2}$		158.2(4)	133.2(7) [−134.2(7)][f]	
$\chi 2^{1,2}$		175.4(3)	57.1(6) [160.0(7)][f]	
$\chi 4^{1,1}$				56.7(5)
$\chi 4^{2,1}$				135.0(7)
$\chi 4^{3,1}$				−62(2)
$\chi 4^{4,1}$				−71(2)
$\chi 4^{5,1}$				145(2)
$\chi 4^{6}$				−96(5)
$\chi 4^{5,2}$				91(3)
$\chi 4^{4,2}$				−64(2)
$\chi 4^{3,2}$				−61.2(19)
$\chi 4^{2,2}$				163.7(6)
$\chi 4^{1,2}$				173.8(4)

[a] N_1–C^{α}_1–C'_1–O_T; [b] N_3–C^{α}_3-C'_3–O_T; [c] C^{α}_3–C'_3–O_T–C_T; [d] N_5–C^{α}_5–C'_5–O_T; [e] C^{α}_5–C'_5–O_T–C_T; [f] The values in parentheses refer to statistically positioned atoms.

Table 4 Intra- and Intermolecular H-bond Parameters for the $Ac_{11}c$ Derivative and Peptides

Compound	Type	Donor	Acceptor	Length (Å) (N···O)	Angle (°) (C′=O···N)	Symmetry operation
Z-$Ac_{11}c$-OH	Intermolecular	N_1	O_1	3.061(3)	136.6(2)	$-x+3/2$, $y-1/2$, $-z+1/2$
		O_T	O_1	2.662(3)	126.5(2)	$2-x$, $1-y$, $1-z$
Z-Aib-$Ac_{11}c$-Aib-O*t*Bu	Intramolecular	N_3A	O_0 A	3.133(3)	129.8(2)	x, y, z
	(1←4)	N_3B	O_0 B	3.043(4)	142.4(2)	x, y, z
	Intermolecular	N_1B	O2A	2.972(3)	163.6(2)	x, y, z
		N_1A	O2B	2.978(3)	153.6(2)	x, y, $1+z$
Z-$Ac_{11}c$-$(Aib)_2$-$Ac_{11}c$-Aib-O*t*Bu	Intramolecular	N_3	O_0	3.020(3)	127.8(3)	x, y, z
	(1←4)	N_4	O_1	2.924(6)	133.4(3)	x, y, z
		N_5	O_2	2.993(6)	131.6(3)	x, y, z
	Intermolecular	N_1	O_4	2.958(8)	137.9(4)	$-1+x$, y, z

cycloundecylmethyl 1-naphthylcarbamate at 293 K [38], the only compound with a system of 11 sp^3 carbon atoms the structure of which has been solved by X-ray diffraction. In particular, the average C–C bond length for the cycloundecyl ring is 1.51 Å (with the longest average distance of 1.66 Å for the $C^{\zeta 1}$–$C^{\zeta 2}$ bond and the shortest average distance of 1.40 Å for the $C^{\varepsilon 1}$–$C^{\zeta 1}$ bond), in good accord with the literature average value of 1.52 Å for the $-CH_2-CH_2-$ length [39]. The values for the N–C^{α}, C^{α}–C′, and C′=O bond lengths fit nicely with the corresponding values for peptides based on protein amino acids [36,37]. The average value for the bond angles internal to the 11-membered ring is 115.0°, significantly larger than the regular tetrahedral value (109.5°). In particular, some of them, centred at the $C^{\beta 2}$, $C^{\delta 1}$, $C^{\varepsilon 1}$ and $C^{\varepsilon 2}$ atoms, are remarkably expanded (116–120°). This significant deviation is also due to the large thermal ellipsoids shown by some carbon atoms of the rings.

Table 5 Average Bond Distances and Bond Angles for the $Ac_{11}c$ Residue

	Bond distance (Å)		Bond angle (°)
N–C^{α}	1.463(6)	N–C^{α}–C′	110.0(3)
C^{α}–C′	1.535(4)	$C^{\beta 1}$–C^{α}–$C^{\beta 2}$	113.3(3)
C′–O	1.221(8)	C^{α}–$C^{\beta 1}$–$C^{\gamma 1}$	115.3(4)
C^{α}–$C^{\beta 1}$	1.533(9)	$C^{\beta 1}$–$C^{\gamma 1}$–$C^{\delta 1}$	115.2(5)
$C^{\beta 1}$–$C^{\gamma 1}$	1.523(5)	$C^{\gamma 1}$–$C^{\delta 1}$–$C^{\varepsilon 1}$	116.1(8)
$C^{\gamma 1}$–$C^{\delta 1}$	1.49(1)	$C^{\delta 1}$–$C^{\varepsilon 1}$–$C^{\zeta 1}$	116(1)
$C^{\delta 1}$–$C^{\varepsilon 1}$	1.54(2)	$C^{\varepsilon 1}$–$C^{\zeta 1}$–$C^{\zeta 2}$	111(1)
$C^{\varepsilon 1}$–$C^{\zeta 1}$	1.39(2)	$C^{\zeta 1}$–$C^{\zeta 2}$–$C^{\varepsilon 2}$	114(1)
$C^{\zeta 1}$–$C^{\zeta 2}$	1.66(2)	$C^{\zeta 2}$–$C^{\varepsilon 2}$–$C^{\delta 2}$	120(1)
$C^{\zeta 2}$–$C^{\varepsilon 2}$	1.42(2)	$C^{\varepsilon 2}$–$C^{\delta 2}$–$C^{\gamma 2}$	112.3(7)
$C^{\varepsilon 2}$–$C^{\delta 2}$	1.52(2)	$C^{\delta 2}$–$C^{\gamma 2}$–$C^{\beta 2}$	112.9(5)
$C^{\delta 2}$–$C^{\gamma 2}$	1.58(1)	$C^{\gamma 2}$–$C^{\beta 2}$–C^{α}	119.0(4)
$C^{\gamma 2}$–$C^{\beta 2}$	1.464(9)	N–C^{α}–$C^{\beta 1}$	113.3(3)
$C^{\beta 2}$–C^{α}	1.538(9)	N–C^{α}–$C^{\beta 2}$	106.1(3)
		C′–C^{α}–$C^{\beta 1}$	102.8(3)
		C′–C^{α}–$C^{\beta 2}$	107.2(3)

In addition, the bond angles indicate an asymmetric geometry for the C^{α} atom. More specifically, the bond angles involving the $C^{\beta 1}$ atom are narrower than those involving the $C^{\beta 2}$ atom. This observation is common to Aib and Ac_nc-rich peptides [14,22]. The average value for the conformationally sensitive N–C^{α}–C′ (τ) bond angle, external to the cyclic system, is 110.0°, comparable to that exhibited by the $C^{\alpha,\alpha}$-disubstituted glycines forming regular bends and helices (110–111°) [14,22,40].

All five $Ac_{11}c$ residues (by taking into account both independent molecules of the tripeptide) are found in the helical region A (A*) of the conformational map [41]. The average value for the ϕ, ψ backbone torsion angles of the $Ac_{11}c$ residue completely involved in a bend/helical structure are $\pm 55.7°$, $\pm 32.7°$, close to those expected for a 3_{10}-helix ($\pm 57°$, $\pm 30°$) [20].

The -Aib-$Ac_{11}c$- sequence of both molecules **A** and **B** of the tripeptide is folded in a 1←4 C=O···H–N intramolecularly H-bonded type III(III′) β-bend conformation. The intramolecular $N_3\cdots O_0$ separation is 3.133(3) Å for molecule **A** and 3.043(4) Å for molecule **B**, within the limits expected for such H-bonds [42–44]. The major backbone conformational difference between molecules **A** and **B** is the

opposite screw sense of the helical β-bend, left-handed for molecule **A** and right-handed for molecule **B**. The 1–4 sequence of the pentamer forms a 3_{10}-helix [three consecutive type III(III′) β-bend conformations] stabilized by three $1 \leftarrow 4$ C=O···H–N intramolecular H-bonds of normal length. In molecules **A** and **B** of the tripeptide and in the pentapeptide also the *C*-terminal Aib residue adopts a conformation in the helical region, but it has an handedness opposite to that shown by the preceding residues, a common observation for helical Aib peptides [14].

In the four molecules only two significant deviations of the ω torsion angles ($|\Delta\omega| > 7.5°$) from the ideal value of the *trans* planar urethane, peptide and ester units (180°) are observed: the urethane ω_0 value of molecule **A** and the peptide ω_2 value of molecule **B** of the tripeptide, which differ by 9.6° and 9.3°, respectively, from the *trans* planar value. The *trans* arrangement of the θ^1 torsion angle of the benzyloxycarbonylamino moiety, found for all of the four molecules of the Z-protected $Ac_{11}c$ derivative and peptides, is that usually exhibited by Z-amino acids and peptides [34]. Not surprisingly, the values of θ^2 are concentrated in three regions, viz. $90 \pm 15°$, $-90 \pm 9°$, and $180 \pm 16°$. In all three peptide molecules the *tert*-butyl ester conformation with respect to the preceding C^{α}–N bond is intermediate between the *anticlinal* and the *anti-periplanar* conformations [45].

A comparison of the torsional angles for the 11-membered rings experimentally found in this work with the force-field torsion angles calculated for the six low-energy conformations of cycloundecane [46–50] shows that the ring tends to assume only two different conformations (Figure 6). In particular, these conformations are essentially identical to the [335] and [12323] conformations discussed by Anet and Rawdah [48], that represent the lowest energy conformations. The [335] conformation of cycloundecane can be considered as derived from the square [3333] conformation of cyclododecane by ring contraction, whereas the [12323] conformation is derivable from the [2323] conformation of cyclodecane by ring expansion [48]. In particular, in each of the $Ac_{11}c$ residues in the [335] conformation (i.e. in both statistic conformations of Z-$Ac_{11}c$-OH, in molecule **A** of the tripeptide, and in residue 4 of the pentapeptide) the endocyclic side-chain χ torsion angles have the following set of average values: ∓ 157.3, $\pm 64.2°$, $\pm 66.4°$, $\mp 142.8°$, $\pm 63.5°$, $\pm 67.7°$, $\mp 123.5°$, $\pm 124.8°$, $\mp 127.8°$, $\pm 65.6°$, and $\pm 63.0°$. On the other hand, in the $Ac_{11}c$ residues in the [12323] conformation these dihedral angles have the following set of average values: $\mp 141.1°$, $\pm 88.3°$, $\mp 89.1°$, $\pm 148.2°$, $\mp 59.5°$, $\mp 84.3°$, $\pm 81.0°$, $\pm 58.5°$, $\mp 150.8°$, $\pm 61.4°$, and $\pm 69.1°$. The major differences with respect to the Anet and Rawdal's conformations [48] are found in the region of the ring far from the C^{α} atom, where there are large thermal ellipsoids. A comparison of these data with the crystal state structure of cycloundecylmethyl 1-naphthylcarbamate [38] and the NMR conformational studies on cycloundecane [47,48] reveals that the two conformations found in the present study are similar to those exhibited by the other compounds reported in literature.

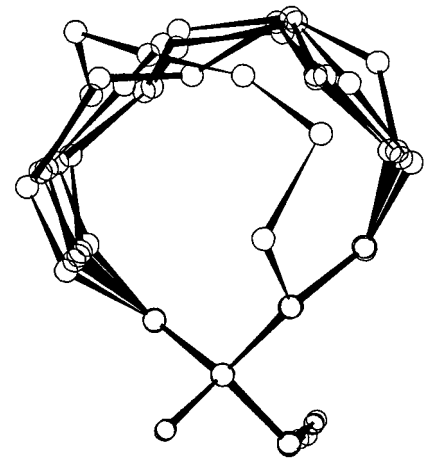

Figure 6 Overlay of the $Ac_{11}c$ cycloaliphatic ring derived from the X-ray diffraction structures discussed in this work.

An additional point of interest is the occurrence in each $Ac_{11}c$ ring of two consecutive χ torsion angles with the same absolute value of $\cong 60°$. This arrangement is responsible for the larger separation between carbon atoms at relative positions 1:5, concomitantly offering enough space to the additional carbon atoms to complete the cyclic structure.

In addition, it is worth noting that for all residues the $\chi^{1,1}$ and $\chi^{1,2}$ side-chain torsion angles are in the (t, g^+) and (t, g^-) conformations for right-handed and left-handed $Ac_{11}c$ residues, respectively. The only exception is found for one of the statistical conformation of the molecule **B** of the tripeptide that presents $\chi^{1,1}$ and $\chi^{1,2}$ side-chain torsion angles in the (g^-, g^+) conformation.

The packing mode of the Z-$Ac_{11}c$-OH molecules is characterized by (carboxylic acid) O_T–H···O_1=C'_1 (carboxylic acid) intermolecular H-bonds, giving rise

to dimeric structures and by (urethane) N_1–H···O_1=C'_1 (carboxylic acid) intermolecular H-bonds forming rows along the *b* direction. The geometrical parameters for the N–H···O [42–44] and O–H···O [51,52] intermolecular H-bonds are in the ranges expected for such interactions.

The packing mode of Z-Aib-$Ac_{11}c$-Aib-O*t*Bu tripeptide, with two independent molecules (**A** and **B**) in the asymmetric unit, is characterized by two (urethane) N–H···O=C(peptide) intermolecular H-bonds [N_{1A}–H···O_{2B}=C'_{2B}, and N_{1B}–H···O_{2A}=C'_{2A}]. These intermolecular interactions, occurring along the *c* direction, link together **A** and **B** molecules in a head-to-tail fashion, thus producing rows of **A**-to-**B** H-bonded peptide molecules. Hydrophobic interactions held together rows of peptides in the other directions.

The Z-$Ac_{11}c$-$(Aib)_2$-$Ac_{11}c$-Aib-O*t*Bu molecules pack together along the *a* direction, producing rows of molecule stabilized by (urethane) N–H···O=C (peptide) intermolecular H-bonds [N_1–H···O_4=C'_4]. In addition, hydrophobic interactions link together rows of peptide molecules running in the *b* and *c* directions.

CONCLUSIONS

Overall, the solution and crystal-state data collected in this work for the $Ac_{11}c$-based peptides are consistent with the contention that this medium-ring cycloaliphatic $C^{\alpha,\alpha}$-disubstituted glycine is structurally constrained and tends to exhibit ϕ, ψ backbone torsion angles characteristic of the 3_{10}-/α-helical region of the Ramachandran map [41]. Therefore, the $Ac_{11}c$ residue can exert a conformational bias in favour of the type III(III′) β-bend (where it may occupy either position $i+1$ or $i+2$) and the type I(I′) β-bend (where it may occupy position $i+1$). It may also be located, although with some energy cost, at position $i+2$ of either type I(I′) or type II(II′) β-bend. Interestingly however, the set of ϕ, ψ torsion angles compatible with the *semi*-extended position $i+1$ of type II(II′) β-bend seems to be precluded to $Ac_{11}c$.

Recently, we have proposed that the series of Ac_nc ($n=3$–12) residues, having increasing effective volume and hydrophobicity but possessing a similar conformational preference, may represent a sound basis for an 'Ac_nc scan' [53]. Actually, we believe that the SAR data of analogues of relevant bioactive peptides, incorporating this whole series of Ac_nc residues at a selected position, may be of great value in delineating the nature of the receptor-bound conformation and in the production of highly active agonists and antagonists. Recently, based on this concept, García-Echevarría *et al.* [54] have elegantly mapped the X_{+1} binding site of the Grb2-SH2 domain. Detailed information on the synthesis, characterization and conformational properties of $Ac_{10}c$ [23], the last residue of this series to be investigated, will be reported soon.

Acknowledgements

The authors gratefully acknowledge MURST, the Ministry of University and of the Scientific and Technological Research, and the National Research Council, CNR, of Italy, for their continuous support to this research. The authors thank Mr. Giuseppe Perretta for technical assistance and Mrs. Linda Sorbilli for typing the manuscript.

REFERENCES

1. Spatola A. Peptide backbone modifications: a structure–activity analysis of peptides containing amide bond surrogates. Conformational constraints, and related backbone modifications. In *Chemistry and Biochemistry of Amino Acids, Peptides, and Proteins*, vol. 7, Weinsten B (ed.). Dekker: New York, 1983; 267–357.
2. Aubry A, Boussard G, Cung MT, Marraud M, Vitoux B. Modulations conformationnelles du repliement β en série peptidique et pseudopeptidique. *J. Chim. Phys. (Fr.)* 1988; **85**: 345–359.
3. Hruby VJ, Al-Obeidi F, Kazmierski W. Emerging approaches in the molecular design of receptor-selective peptide ligands: conformational, topographical and dynamic considerations. *Biochem. J.* 1990; **268**: 249–262.
4. Toniolo C. Conformationally restricted peptides through short-range cyclizations. *Int. J. Peptide Protein Res.* 1990; **35**: 287–300.
5. Holzemann G. Peptide conformation mimetics, 1991. *Kontakte (Darmstadt)*, 3–12 (part 1) and 55–63 (part 2).
6. Giannis A, Kolter T. Peptidomimetics for receptor ligands. Discovery, development, and medical perspectives. *Angew. Chem. Int. Ed. Engl.* 1993; **32**: 1244–1267.
7. Adang AEP, Hermkens PHH, Linders JTM, Ottenheijm HCJ, van Staveren CJ. Case histories of peptidomimetics: progression from peptides to drugs. *Recl. Trav. Chim. Pays-Bas* 1994; **113**: 63–78.
8. Gante J. Peptidomimetics: tailored enzyme inhibitors. *Angew. Chem. Int. Ed. Engl.* 1994; **33**: 1699–1720.

9. Liskamp RMJ. Conformationally restricted amino acids and dipeptides, (non)peptidomimetics and secondary structure mimetics. *Recl. Trav. Chim. Pays-Bas* 1994; **113**: 1–19.
10. Hanessian S, Mc Naughton-Smith G, Lombart H-G, Lubell WD. Design and synthesis of conformationally constrained amino acids as versatile scaffolds and peptide mimetics. *Tetrahedron* 1997; **53**: 12789–12854.
11. Ishida H, Inoue Y. Peptides that contain unnatural amino acids: toward artificial proteins. *Rev. Heteroatom Chem.* 1999; **19**: 79–142.
12. Marshall GR. Studies on the biologically active conformations of angiotensin. In *Intra-Science Chemistry Report*, Kharasch N (ed.). Gordon and Breach: New York, 1971; 305–316.
13. Karle IL, Balaram P. Structural characteristics of α-helical peptide molecules containing Aib residues. *Biochemistry* 1990; **29**: 6747–6756.
14. Toniolo C, Benedetti E. Structures of polypeptides from α-amino acids disubstituted at the α-carbon. *Macromolecules* 1991; **24**: 4004–4009.
15. Karle IL. Aspects of peptide folding and aggregation. *Acc. Chem. Res.* 1999; **32**: 693–701.
16. Kaul R, Balaram P. Stereochemical control of peptide folding. *Bioorg. Med. Chem.* 1999; **7**: 105–117.
17. Venkatachalam CM. Stereochemical criteria for polypeptides and proteins. V. Conformation of a system of three-linked peptide units. *Biopolymers* 1968; **6**: 1425–1436.
18. Toniolo C. Intramolecularly hydrogen-bonded peptide conformations. *CRC Crit. Rev. Biochem.* 1980; **9**: 1–44.
19. Rose GD, Gierasch LM, Smith JP. Turns in peptides and proteins. *Adv. Protein Chem.* 1985; **37**: 1–109.
20. Toniolo C, Benedetti E. The polypeptide 3_{10}-helix. *Trends Biochem. Sci.* 1991; **16**: 350–353.
21. Toniolo C, Crisma M, Formaggio F, Benedetti E, Santini A, Iacovino R, Saviano M, Di Blasio B, Pedone C, Kamphuis J. Preferred conformation of peptides rich in alicyclic $C^{\alpha,\alpha}$-disubstituted glycines. *Peptide Sci. (Biopolymers)* 1996; **40**: 519–522.
22. Moretto V, Formaggio F, Crisma M, Bonora GM, Toniolo C, Benedetti E, Santini A, Saviano M, Di Blasio B, Pedone C. Preferred conformation of peptides rich in Ac_8c, a medium-ring alicyclic $C^{\alpha,\alpha}$-disubstituted glycine. *J. Peptide Sci.* 1996; **2**: 14–27.
23. Benedetti E, Saviano M, Iacovino R, Crisma M, Formaggio F, Toniolo C. Peptide folding as a result of the incorporation of large-ring, cyclophatic $C^{\alpha,\alpha}$-disubstituted glycines. In *Peptides for the New Millennium*, Fields GB, Tam JP, Barany G (eds). Kluwer Academic: Dordrecht, The Netherlands, 2000 (in press).
24. Altomare A, Burla MC, Camalli M, Cascarano G, Giacovazzo C, Guagliardi A, Moliterni AGG, Polidori G, Spagna R. *A Program for Automatic Solution and Refinement of Crystal Structures*. University of Bari: Bari, Italy, 1997.
25. Sheldrick GM. *SHELXL97. Program for Crystal Structure Refinement*. University of Göttingen: Göttingen, Germany, 1997.
26. Cromer DT, Waber JT. *International Tables for X-Ray Crystallography*, vol. IV. Kynoch Press: Birmingham, UK, 1974. Table 2.2 B (now distributed by D. Reidel: Dordrecht, Netherlands).
27. Treleano R, Belitz HD, Jugel H, Wieser H. Beziehungen zwisches Struktur und Geschmack bei Aminosäuren mit cyclischen Seitenketten. *Z. Lebensm. Unters. Forsch.* 1978; **167**: 320–323.
28. Carpino LA. 1-Hydroxy-7-azabenzotriazole. An efficient peptide coupling additive. *J. Am. Chem. Soc.* 1993; **115**: 4397–4398.
29. Bonora GM, Mapelli C, Toniolo C, Wilkening RR, Stevens ES. Conformation analysis of linear peptides: 5. Spectroscopic characterization of β-turns in Aib-containing oligopeptides in chloroform. *Int. J. Biol. Macromol.* 1984; **6**: 179–188.
30. Kopple KD, Ohnishi M. Conformations of cyclic peptides. IV. Nuclear magnetic resonance studies of cyclopentaglycyl-L-leucyl and cyclodiglycyl-L-histidyl-diglycyl-L-tyrosyl. *Biochemistry* 1969; **8**: 4087–4095.
31. Martin D, Hauthal HG. *Dimethyl Sulphoxide*. Van Nostrand-Reinhold: Wokingham, UK, 1975.
32. Kopple KD, Schamper TJ. Proton magnetic resonance line broadening produced by association with a nitroxide radical in studies of amide and peptide conformation. *J. Am. Chem. Soc.* 1972; **94**: 3644–3646.
33. IUPAC-IUB Commission on Biochemical Nomenclature. Abbreviations and symbols for the description of the conformation of polypeptide chains. *Biochemistry* 1970; **9**: 3471–3479.
34. Benedetti E, Pedone C, Toniolo C, Dudek M, Némethy G, Scheraga HA. Preferred conformation of the benzyloxycarbonyl-amino group in peptides. *Int. J. Peptide Protein Res.* 1983; **21**: 163–181.
35. Schweizer WB, Dunitz JD. Structural characteristics of the carboxylic ester group. *Helv. Chim. Acta.* 1982; **65**: 1547–1554.
36. Benedetti E. Structure and conformation of peptides as determined by X-ray crystallography. In *Chemistry and Biochemistry of Amino Acids, Peptides, and Proteins*, vol. 6, Weinstein B (ed.). Dekker: New York, 1982; 105–184.
37. Ashida T, Tsunogae Y, Tanaka I, Yamane T. Peptide chain structure parameters, bond angles and conformational angles from the Cambridge structural database. *Acta Crystallogr.* 1987; **B43**: 212–218.
38. Russell MA, Sim GA. Dynamic conformational behaviour of an eleven-membered ring in the solid state. X-Ray studies of cycloundecylmethyl 1-naphthylcarbamate at 120 and 293 K. *Acta Crystallogr.* 1990; **B46**: 671–675.
39. Allen FH, Kennard O, Watson DG, Brammer L, Orpen AG, Taylor R. Tables of bonds lengths determined by X-ray and neutron diffraction. Part 1. Bond lengths in organic compounds. *J. Chem. Soc. Perkin Trans. 2* 1987; S1–S19.

40. Paterson Y, Rumsey SM, Benedetti E, Némethy G, Scheraga HA. Sensitivity of polypeptide conformation to geometry. Theoretical conformational analysis of oligomers of α-aminoisobutyric acid. *J. Am. Chem. Soc.* 1981; **103**: 2947–2955.
41. Zimmerman SS, Pottle MS, Némethy G, Scheraga HA. Conformational analysis of the 20 naturally occurring amino acid residues using ECEPP. *Macromolecules* 1977; **10**: 1–9.
42. Ramakrishnan C, Prasad N. Study of hydrogen bonds in amino acids and peptides. *Int. J. Protein Res.* 1971; **3**: 209–231.
43. Taylor R, Kennard O, Versichel W. The geometry of the N–H···O=C hydrogen bond. 3. Hydrogen-bond distances and angles. *Acta Crystallogr.* 1984; **B40**: 280–288.
44. Görbitz CH. Hydrogen-bond distances and angles in the structures of amino acids and peptides. *Acta Crystallogr.* 1989; **B45**: 390–395.
45. Dunitz JD, Strickler P. Preferred conformation of the carboxyl group. In *Structural Chemistry and Molecular Biology*, Rich A, Davidson N (eds). Freeman: San Francisco, 1968; 595–602.
46. Bixon M, Lifson S. Potential functions and conformations in cycloalkanes. *Tetrahedron* 1967; **23**: 769–784.
47. Anet FAL, Cheng AK, Wagner JJ. Determination of conformational energy barriers in medium- and large-ring cycloalkanes by ^{1}H and ^{13}C nuclear magnetic resonance. *J. Am. Chem. Soc.* 1972; **94**: 9250–9252.
48. Anet FAL, Rawdah TN. Iterative force-field calculations of cycloundecane, cyclotridecane, and cyclopentadecane. *J. Am. Chem. Soc.* 1978; **100**: 7810–7814.
49. Kolossvary I, Guida WC. Comprehensive conformational analysis of the four- to twelve-membered ring cycloalkanes: identification of the complete set of interconversion pathways on the MM2 potential energy hypersurface. *J. Am. Chem. Soc.* 1993; **115**: 2107–2119.
50. Weinberg N, Wolfe S. A comprehensive approach to the conformational analysis of cyclic compounds. *J. Am. Chem. Soc.* 1994; **116**: 9860–9868.
51. Brown ID. On the geometry of O–H···O hydrogen bonds. *Acta Crystallogr.* 1976; **A32**: 24–31.
52. Mitra J, Ramakrishnan C. Analysis of O–H···O hydrogen bonds. *Int. J. Peptide Protein Res.* 1977; **9**: 27–48.
53. Saviano M, Iacovino R, Menchise V, Benedetti E, Bonora GM, Gatos M, Graci L, Formaggio F, Crisma M, Toniolo C. Conformational restriction through $C_i^{\alpha} \leftrightarrow C_i^{\alpha}$ cyclization: $Ac_{12}c$, the largest cycloaliphatic $C^{\alpha,\alpha}$-disubstituted glycine known. *Biopolymers* 2000; **53**: 200–212.
54. García-Echevarría C, Gay B, Rahuel J, Furet P. Mapping the X_{+1} binding site of the Grb2-SH2 domain with α,α-disubstituted cyclic α-amino acids. *Bioorg. Med. Chem. Lett.* 1999; **9**: 2915–2920.

